Non-linear Aeroelastic Formulation And Validation Using Nasa Hirenasd Experimental And Computational Simulation Data

[1]M.Vinoth, [2]I.Rajendran
Department of Mechanical Engineering
Dr.Mahalingam College of Engineering and Technology
Pollachi, INDIA

***Abstract* - A series of aeroelastic analyses is performed for a flexible high-aspect-ratio wing of typical civil aircraft configuration. Those aircrafts are lead to dynamic instabilities such as flutter, which can cause large amplitude limit cycle oscillations. The nonlinear aero elastic formulation and the Eigen value based solution is validated by using NASA Aeroelastic prediction workshop, Aero-structural dynamical experiments with an elastic wing model which are conducted during the High Reynolds Number Aero-Structural Dynamics (HIRENASD) project by RWTH Aachen University in the cryogenic European Transonic Windtunnel. Quasi-steady aerodynamic theory has been used to model the aerodynamic forces and the model is considered as fluid-solid interaction problem. Such model is first solved with the CFD solver and it is coupled with FEA, to predict the aero-elastic phenomena at transonic flight regime for various common materials used in airplanes. The various aero elasticity design parameters of Aerodynamic, Inertia and Structural aspects will be validated through computational simulation data of HIRENASD model for aero-elasticity behaviors.**

***Keywords* - Aero-elasticity, HIRENASD, Fluid-Structure interaction problem.**

I. INTRODUCTION

As a structure moves through the air, the motion will cause aerodynamic loads, leading to deformations of the structure. The deformation affects the airflow, thus there is change in the aerodynamic loading. Furthermore there is a closed relation of structural and aerodynamic interactions, and depending on the properties of the structure and the airflow, different phenomena can occur. Such phenomena is commonly known as aeroelastic phenomena and it deals with the aeroelasticity of the structures or structural dynamics. Only very few aeroelastic windtunnel experiments have been performed with oscillating elastic aircraft wings in the transonic flow regime at flight Reynolds numbers of large transport aircrafts.

For an airfoil in transonic flow with prescribed oscillation buffet has been examined at high Reynolds number in a cryogenic environment at NASA Langley Research Center[1,2].The aeroelastic windtunnel experiments with elastic wings at high Reynolds numbers are necessary for validating methods of multidisciplinary airplane design and for realistic Computational Aero-Structural Dynamics (CASD) simulation of airplanes in flight.

Thus the objectives of this paper is to gain better aero-structural dynamics understanding and knowledge about the fluid- structure interaction at airplane wings in the transonic regime in a wide range of Reynolds numbers and aerodynamic loads for current and future aerodynamic and aeroelastic research.

The HIRENASD project was initiated within the Collaborative Research Centre SFB401 at RWTH Aachen University with funding by the German Research Foundation(DFG) in 2004. High Reynolds number ASD experiments were successfully conducted with an elastic supercritical wing in November 2006 in the European Transonic Windtunnel (ETW). The aeroelastic behavior of the wing model was studied during steady polar at slowly varying angle of attack and during dynamic aeroelastic tests at fixed root angle of attack under vibration excitation in the wing root region. In this paper selected conditions of this experiment were taken and software based analysis were done.

II. THE HIRENASD WIND TUNNEL MODEL

The HIRENASD (High REynolds Number Aero Structural Dynamics) wing model corresponds to the SFB 401 clean wing reference configuration with a plan view typical for wings of high speed transport

aircrafts. It is a wing model with a semispan of almost 1.30m, an aerodynamic mean chord of 0.3445m, a constant leading edge sweep of 34^o and a trailing edge with two kinks, segmenting the wing into three spanwise sections[1]. The aerodynamic profile of the wing is defined according to the supercritical BAC 3-11/RES/30/21. The relative thickness in the innermost section I changes span wise conically from 15% to 11%, whereas in both outer sections the relative thickness remains constant at 11% as shown in Fig 2. To permit good access to the internal instrumentation, the wing is composed of two bolted shells made of VascomaxC-200. This special steel is optimized for use under cryogenic conditions. Its Young's modulusexhibits a temperature dependence given as $E=190.3GPa-0.0416GPa/K(T-77K)$.

The model was arranged hanging from the wind tunnel ceiling into the test section ofETW. To reduce the influence of the boundary layer developing along the ceiling, a fuselage substitute was designed. It is fixed on the wind tunnel turntable without having any mechanical contact with the wing and being designed very stiff. The aerodynamically relevant part of the HIRENASD model is depicted in Fig. 1 as is placed in ETW's test section.

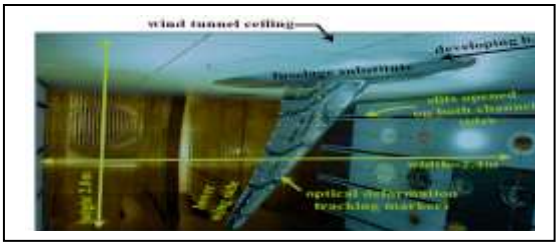

Fig. 1. Experimental wing model in EuropeanTransonic Wind tunnel.

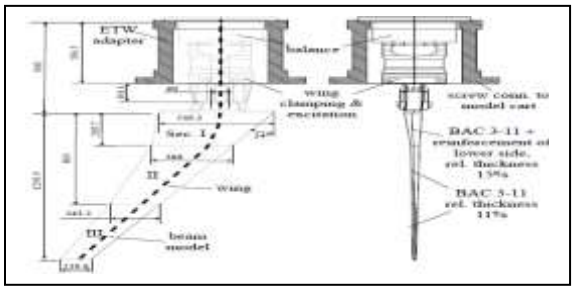

Fig. 2. Wing model drawing.

The supporting part of the HIRENASD model, which is located above the wind tunnel ceiling, is designed as follows: The wing model is mounted on a piezo-electrical 6- components balance which is specifically tailored to the needs of dynamic force recording during HIRENASD experiments. The full assembly is connected to ETW's model cart with a cylindrical adapter and thereby prepared to be placed in the measuring section of ETW as for half-model testing. To enable dynamic aero-elastic experiments, force couples acting in span wise direction can be applied to the wing root plane by a vibrational excitation mechanism which is housed inside the wing clamping device. The latter is connected to the balance by a cylindrical shell.

III. AERO-ELASTIC BEHAVIOR OF THE PRESSURE DISTRIBUTION ON CFD ANALYSIS

Since backward-swept wings experience a span wise reduction of local angles of attack. When being bent upwards, their integral lift coefficient is always lower than for a wing without any deformation. This behavior becomes also apparent for the HIRENASD wing. For Mach numbers 0.80 the improvement with respect to experimental results by considering model deformation is significant. The streamline patterns displayed in combination with c_p distributions about AECs at different materials, viz., maraging steel, aluminum alloy and structural steel at Mach number 0.80 enable insight show the wing deformation interacts with the flow separation. For Ma=0.80 the flow is detached for the two outer wing sections if a rigid wing is assumed. This challenging flow situation may cause the deviations in lift which arise

between simulation and experiment for Ma=0.80.

Fig. 3. CFD wing model.

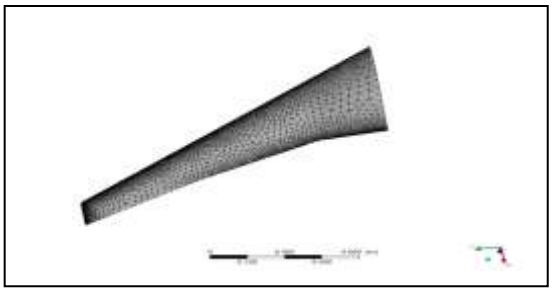

Fig. 4. CFD Mesh.

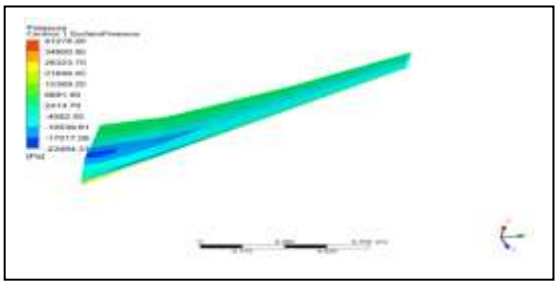

Fig. 5. Pressure distribution around the wing surface.

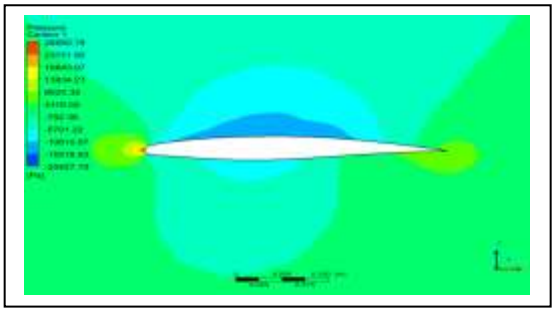

Fig. 6. Pressure distribution around wing cross section.

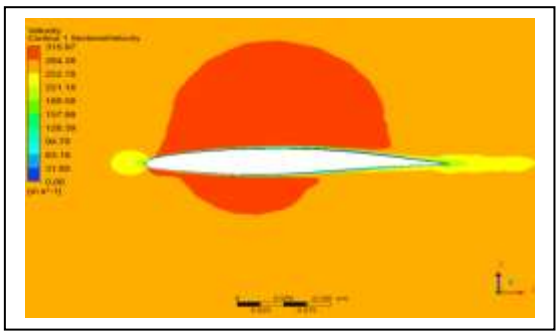

Fig. 7. Velocity contour around wing cross section.

A strong shock occurring where the airfoil is thickened from originally 11% to 15% relative thickness in the inner section on the lower wing sideas shown in Fig 6 and 7. In addition, a separation region is present at negative α shortly behind the characteristic turning point in the nose region of the BAC- 3/11 airfoil on the lower side, even for low Mach numbers.

IV.AERO STRUCTURAL COUPLING OF CFD AND FEA

Since this is the fluid- structure interaction problem, it is necessary to couple both the CFD and FEA to obtain the aero-elastic behavior of the wing structure. For this, the geometries of CFD and FEA are modeled separately as shown in Fig. 3. The CFD model is meshed as shown in Fig. 4 and flow analysis is made on this model with the boundary conditions of Mach 0.80 and angle of attack kept for 0^{o} on ANSYS Fluent solver. The model used to solve is viscous- k omega (2eqns) in order to capture the flow separation and pressure distribution around the

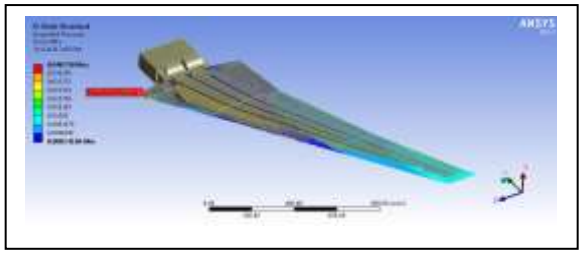

wingsurface due to the airflow.

Fig. 8. Imported pressure around wing structure.

The results of the flow analysis is taken as pressure distribution and it is made to couple with FEA model as the varying pressure load around the wing surface as shown in Fig. 8. Then the FEA model with applied pressure load is solved for modal analysis to obtain the different modes of about 10 modes.

TABLE I. BOUNDARY CONDITIONS GIVEN AND CORRESPONDING RESULTS.

Materials used	Mach	Angle of attack (deg)	Excitat-ion freque-ncy (Hz)	Correspo nding maximu m amplitud e (mm)
Maraging steel	0.8	0	48.879	13.566
Aluminum alloy	0.8	0	47.814	22.896
Structural steel	0.8	0	47.89	13.565

V. DYNAMIC PROPERTIES OF STRUCTURAL MODEL

A. Excitation of 1st Flap-Bending Dominated Mode

The wing was excited to vibrate in its 1st flap-bending dominated mode by subjecting the structure to an equilibrium group of two bending moments. These oscillated according to the parameters given in the first row of Table 1. The maximum flap-bending frequency for Maraging steel, Aluminum alloy and Structural steel were126.93 Hz, 124.26 Hz, and 124.4 Hz respectively and amplitudes for Maraging steel, Aluminum alloy and Structural steel were 20.75mm, 34.969mm, 20.741mm respectively at the wing tip. The bending mode shapes for three different materials were shown in Fig. 9,Fig. 10 and Fig. 11.

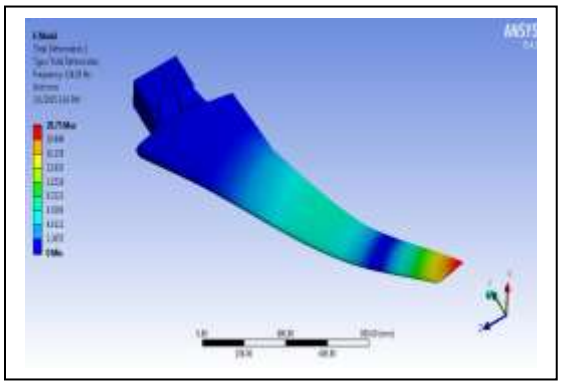

Fig. 9. 1st flap-bending dominated mode shape of wing structure made of Maraging steel.

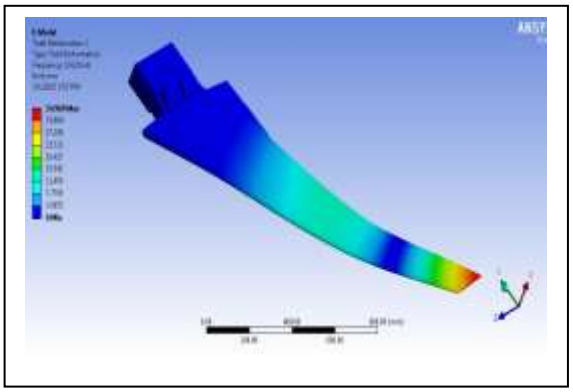

Fig. 10. 1st flap-bending dominated mode shape of wing structure made of Aluminum alloy.

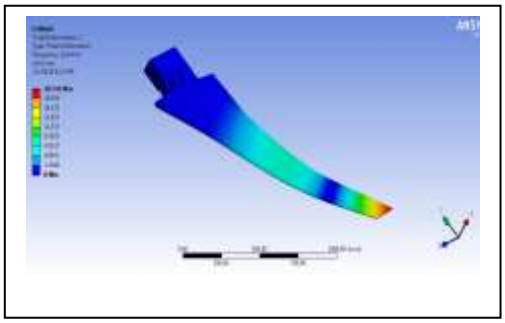

Fig. 11. 1st flap-bending dominated mode shape of wing structure made of Structural steel.

B.Excitation of 2nd Flap-Bending Dominated Mode

The parameters of the second row of Table. 1 were set to excite the 2nd flap-bending dominated Mode in the simulation. The maximum flap-bending frequency for Maraging steel, Aluminum alloy and Structural steel were 247.2 Hz, 242.69 Hz, and 242.5 Hz respectively and amplitudes for Maraging steel, Aluminum alloy and Structural steel were 22.013 mm, 37.099 mm, 22.004 mm respectively at the wing tip. In this case the state of constant vibration amplitudes was reached due to a lower aerodynamic damping of the 2nd mode than previously of the 1st mode. For the same reason, the amplitude of the flap-bending deflection increased. The bending mode shapes for three different materials were shown in Fig.12, Fig. 13 and Fig. 14.

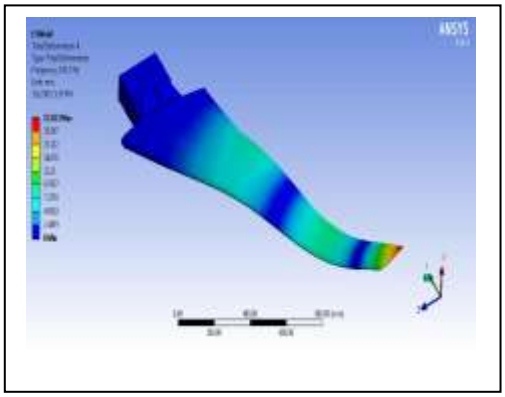

Fig. 12. 2nd flap-bending dominated mode shape of wing structure made of Maraging steel.

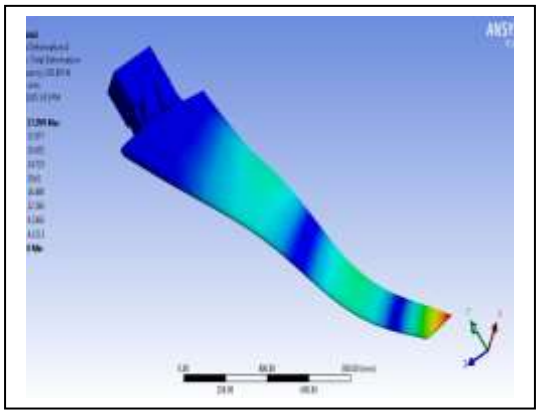

Fig. 13. 2nd flap-bending dominated mode shape of wing structure made of Aluminum alloy.

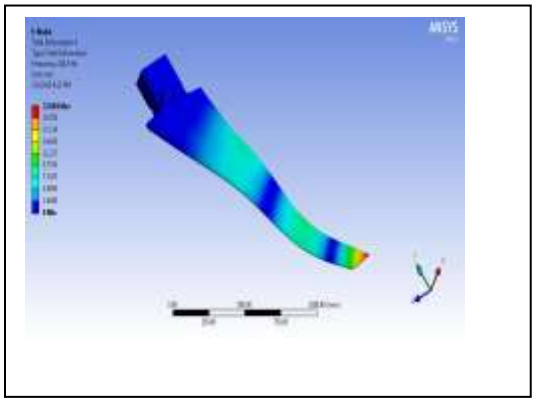

Fig. 14. 2nd flap-bending dominated mode shape of wing structure made of Structural steel.

C. Excitation of 1st Torsion Dominated Mode

The 1st torsion-dominated mode is actually more flap-bending dominated. It was excited by an equilibrium group of bending moments which oscillated according to the parameters of the third row of Tab. 1. The maximum flap-bending frequency for Maraging steel, Aluminum alloy and Structural steel were 336.78 Hz, 329.4 Hz, 330 Hz respectively and amplitudes for Maraging steel, Aluminum alloy and Structural steel were 13.073 mm, 21.9 mm, 13.045 mm respectively at the wing tip. The torsion mode shapes for three different materials were shown in Fig. 15, Fig. 16 and Fig. 17.

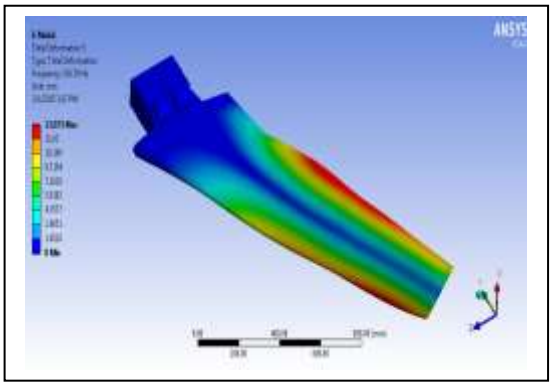

Fig. 15. 1st torsion-dominated mode shape of wing structure made of Maraging steel.

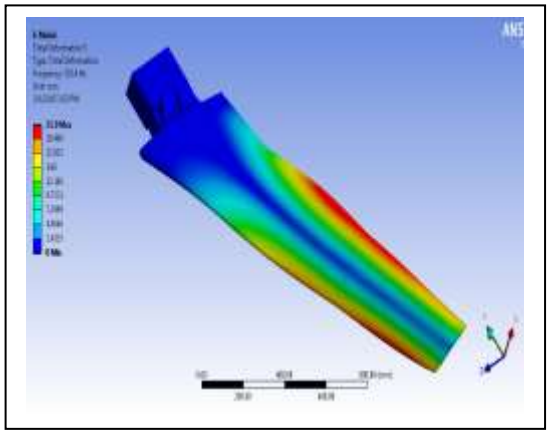

Fig. 16. 1st torsion-dominated mode shape of wing structure made of Aluminum alloy.

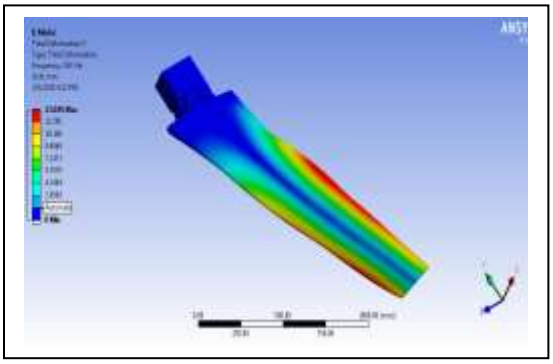

Fig. 17. 1st torsion-dominated mode shape of wing structure made of Structural steel.

VI. CONCLUSION

The structural model identification revealed that Eigen shapes and Eigen frequencies are strongly influenced by the wind tunnel model support. The consideration of the adapter between ETW's model cart and the balance is essential to improve the agreement between computational and experimental Eigen frequencies, and in particular, to obtain a match between computational and experimental Eigen shapes. Comparing experiments with excitation of 1st and 2nd flap-bending modes and their corresponding simulations, a very good agreement of the ratios of unsteady pressure amplitudes and excited accelerations can be stated. The use of the structural model without revision accounts for the slight discrepancy observed for the excitation of the torsional mode. The results obtained for selected excitations are very promising for evaluations and comparisons to be carried out next. These will focus on actual correlations between quantities representing the unsteady aerodynamic interaction in a more integral manner, e.g. the span wise lift distribution, and the structural motion being excited. Further investigations will be made concerning the influences of Mach number and c_p on the ASD of the model.

Although there are slight variations only found in the aero-elastic behavior of different materials used for the elastic wing structure.

REFERENCES

[1] Ballmann," Experimental Analysis of High Reynolds Number Aero-Structural Dynamics in ETW", AIAA Aerospace Sciences Meeting and Exhibit. PP. 1-15, 2008.

[2] Benjamin P. Hallissy, Carlos E.S. Cesnik, "High-fidelity Aeroelastic Analysis of Very Flexible Aircraft", AIAA/ASME/ASCE/AHS/ASC Structures, Structural Dynamics and Materials Conference, American Institute of Aeronautics and Astronautics, PP. 2-22, 2011.

[3] Carlos E. S. Cesnik and Weihua Su, "Nonlinear Aeroelastic Simulation of X-HALE: a Very Flexible UAV", AIAA Aerospace Sciences Meeting including the New Horizons Forum and Aerospace Exposition. PP. 1-13,2011.

[4] Cestino. E ,Frulla G, Romeo.G, "Design of a high-altitude long-endurance solar-powered unmanned air vehicle for multi-payload and operations", JAERO, DOI: 10.1243/09544100, Vol. 221, PP. 199-216,2007.